

Fig. 2. Temperature field and temperature pressure distributions over transverse sections of the jet; t ($^{\circ}\text{C}$); ΔP (mbar); x, y (mm).

The operating channel, formed by interchangeable transparent plates, made of organic glass or LK-7 heat-resistant glass, is located beyond the cut-off. The channel is open at the top and bottom for the inflow of water. The total height of the channel is equal to 0.8 m, while its length is equal to 0.230 m; the height of the water layer above the nozzle is equal to 0.3 m.

From the operating channel, the jet, which now contains condensed vapor, arrives in the outlet channel 5 and flows with a certain head into the mixing tank 1, where controlled mixing with additional cold water from the supply line is effected.

The large open surface area (approximately 2.5 m^2) and the low flow velocity create conditions for considerable deaeration of water, which flows from the mixing tank with the operating tank 2 through the supply channel 6. A constant water level in the operating tank is ensured by overflow through an opening.

Saturated steam at a pressure of approximately 10 bar is throttled in valves 10 and 11 to ensure the operating pressure P_0 in the nozzle forechamber. Before the steam reaches the forechamber, it is saturated at the pressure P_0 by passing it through moistener-receiver 8 and separator 7. The operating chamber in the nozzle chamber varies from 1.3 to 1.7 bar.

The temperature inside and outside the jet is measured by means of two Nichrome-Constantan thermocouples. One thermocouple is fastened to the coordinate spacer 9, while the other is fixed outside the jet and serves for checking periodically the temperature of the water toward flowing the jet. The thermocouple wires have each a diameter of $6 \cdot 10^{-5} \text{ m}$, while the bead diameter is equal to their sum. The wires are placed in a steel syringe needle with an inside diameter of $20 \cdot 10^{-5} \text{ m}$ and an outside diameter of $40 \cdot 10^{-5} \text{ m}$.

The wires are fastened and thermally insulated by filling the space between them and the inside surface of the needle with epoxy resin. The thermocouple bead protrudes $0.7 \cdot 10^{-3} \text{ m}$ from the needle. The thermocouples are calibrated in an oil thermostat by means of a KSP-4 automatic potentiometer. This potentiometer is also used for recording the thermo-emf in performing the experiments. The thermocouple needle is fastened on a blade with a thickness of $3 \cdot 10^{-3} \text{ m}$ and protrudes from its leading stage into the oncoming flow to a distance of $2 \cdot 10^{-3} \text{ m}$.

One side of the blade is tapered to a feather at the leading edge. The other side, which is parallel to the lateral walls of the operating channel, has an opening with a diameter of $0.8 \cdot 10^{-3} \text{ m}$ at a distance of $3 \cdot 10^{-3} \text{ m}$ from the leading edge. The opening is connected to the channel inside the blade and the tube leading to the differential mercury pressure gage.

After the device is switched on, it is left to operate for 30-40 min to provide a warming-up period for the steam supply pipes and establish a steady-state outflow of steam into water at the assigned temperature. The thermocouple is moved by means of a coordinate spacer in steps of $0.5 \cdot 10^{-3} \text{ m}$ over transverse sections of the jet. The section closest to the nozzle is located at a distance of $1 \cdot 10^{-3} \text{ m}$ from the cut-off; the spacing between sections is usually equal to $0.5 \cdot 10^{-3}$ or $1.0 \cdot 10^{-3} \text{ m}$.

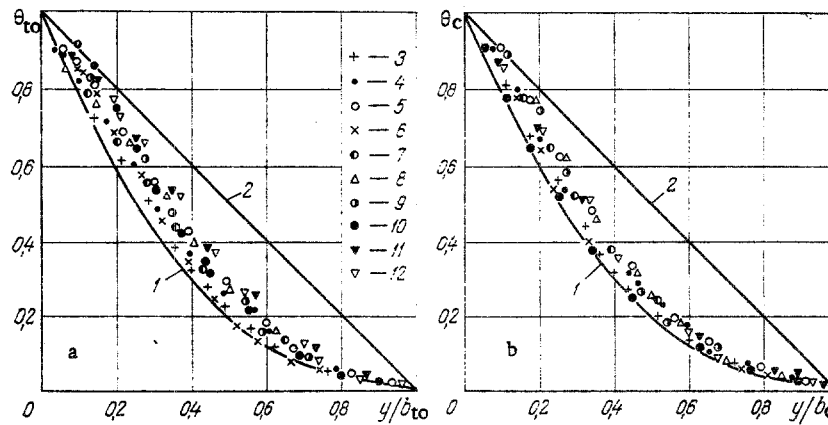


Fig. 3. Temperature distributions: a) $\Theta_{t0} = (t - t_{\infty}) / (t_{in} - t_{\infty})$ in the total thermal mixing layer y/b_{t0} ; b) $\Theta_c = (t - t_{\infty}) / (t_{sin} - t_{\infty})$ in the thermal mixing layer with condensation y/b_c ; 1) after [8]; 2) [7]; 3-5) $P_0 = 1.3$ bar; 3) $t_{\infty} = 14.7^{\circ}\text{C}$; 4) 16.3; 5) 26.5; 6-9) $P_0 = 1.5$ bar; 6) $t_{\infty} = 18.5^{\circ}\text{C}$; 7) 21.2; 8) 27.4; 9) 33.0; 10-12) $P_0 = 1.7$ bar; 10) $t_{\infty} = 21.0^{\circ}\text{C}$; 11) 42.0; 12) 42.3.

Recording at each point by means of the automatic potentiometer is performed over a period of 10-15 sec. While moving the thermocouple, a zero voltage is supplied to KSP-4 for marking the zero point of the instrument.

Using the calibration data for the thermocouple, we determine the coordinates of the points in space with certain temperatures with respect to each thermogram, and then use these data to plot isotherms (Fig. 2). The isotherms plotted for each set of operating conditions are all linear and converge to a single point - the pole II. This indicates the similarity of temperature profiles for transverse sections of the jet which are parallel to each other. We use the following limiting isotherms for the total thermal mixing layer: the inside isotherm t_{in} at the location where the temperatures on the thermogram reach a constant value (in the vapor cone) and the outside isotherm t_{ou1} at the point where the temperature exceeds the water ambient temperature t_{∞} by 0.01 ($t_{in} - t_{\infty}$). The temperature t_{in} is assumed to be equal to the saturation temperature, which corresponds to the steam pressure in the nozzle forechamber. On the basis of the isotherms (Fig. 2), we determine the data for an arbitrary $x = \text{const}$ to plot the relationship (Fig. 3a)

$$\Theta_{t0} = \frac{t - t_{\infty}}{t_{in} - t_{\infty}} = f\left(\frac{y}{b_{t0}}\right).$$

Curve 1 corresponds to the temperature distribution based on the expression [8]

$$\Theta_{t0} = \frac{t - t_{\infty}}{t_{in} - t_{\infty}} = 1 - \frac{2}{\sqrt{\pi}} \int_0^{\eta} \exp(-\alpha^2) d\alpha,$$

where

$$\eta = \eta_{\max} \cdot \frac{y}{b_{t0}}, \text{ while } \eta_{\max} = 1.8215.$$

The straight line 2 corresponds to a linear temperature variation across the thermal mixing layer [5, 7].

A comparison shows qualitative agreement between the theoretical [8] and the experimental data.

We also measured the static pressure in the jet. As an example, Fig. 2 shows the curve of pressure distribution in one of the transverse sections of the jet along with the temperature profile. The steam pressure in the nozzle forechamber was equal to $P_0 = 1.5$ bar, while the temperature of the water ambient was $t_{\infty} = 18.5^{\circ}\text{C}$. The pressure distribution curve indicates that a low-pressure region exists inside the jet. This region encompasses the internal vapor cone and a part of the thermal mixing layer. The development of rarefaction is most probably caused by condensation processes. The maximum degree of rarefaction is encountered in the zone of most intensive condensation. This section corresponds to a layer with a temperature in the range

from 75 to 109°C, which has a thickness of the order of $1 \cdot 10^{-3}$ m. It is possible that a considerable part of the vapor in the core condenses in this thin layer. Subsequently, the pressure increases and almost reaches the ambient pressure in the thermal mixing layer, which is characterized by a thickness of the order of $(1-3) \cdot 10^{-3}$ m and temperatures in the range from 75 to 25°C. It is probable that condensation of all of the steam is completed in this layer.

The saturation temperature corresponding to the pressure in the layer characterized by intensive condensation is, on the average, equal to 98°C for the operating conditions under investigation. We shall use the $t_{s \text{ in}} = 98^\circ\text{C}$ isotherm as the boundary isotherm for the thermal mixing layer with condensation. For the outside boundary of the mixing layer, we shall use the isotherm at which the temperature $t_{s \text{ ou}}$ exceeds the temperature of the water ambient t_∞ by 0.01 ($t_{s \text{ in}} - t_\infty$):

$$t_{s \text{ ou}1} = t_\infty + 0,01 (t_{s \text{ in}} - t_\infty).$$

Figure 3b shows the dimensionless temperature $\Theta_c = (t - t_\infty) / (t_{s \text{ in}} - t_\infty)$ as a function of y/b_c for the investigated steam outflow conditions.

The theoretical curves 1 and 2 are the same as in Fig. 3a. Comparison shows that the experimental points in Fig. 3b are characterized by a lower degree of scatter and that they lie closer to curve 1 than in Fig. 3a. This suggests that following conclusions:

- 1) The theoretical relationship proposed in [8] is in satisfactory agreement with experimental data;
- 2) the equilibrium isotherm with respect to the minimum pressure in the jet can be used as the inside boundary of the mixing layer;
- 3) for the half-thickness of the thermal mixing layer ($y/b_c = 0.5$), the variation of the relative temperature Θ_c is approximately linear:

$$\Theta_c = \frac{t - t_\infty}{t_{s \text{ in}} - t_\infty} = 1 - 1.6 \frac{y}{b_c},$$

while $y/b_c = 0.5$ for $\Theta_c = 0.20$.

These conclusions hold for a fully developed turbulent thermal mixing layer. At the very edge of the nozzle, the development of the initial section of the thermal mixing layer [over a distance on the order of $(1-2) \cdot 10^{-3}$ m from the nozzle edge K (Fig. 2)] is affected by intensive steam and liquid shoots thrown out to both sides of the mixing layer, which leads to virtually stepwise increments in its thickness. Therefore, the pole II to which the straight-line isotherms of the thermal mixing layer converge, is not located at the outlet edge K of the nozzle, but is shifted to the left and slightly upward. Further investigations are necessary for determining the condensing jet geometry and the position of pole II.

NOTATION

x	is the coordinate axis coinciding with the inside boundary isotherm t_{in} or $t_{s \text{ in}}$ of the thermal mixing layer;
y	is the coordinate axis perpendicular to the x axis;
X/H and Y/H	are the dimensionless coordinates directed along the jet axis and perpendicular to it, respectively;
H	is the nozzle height at the outlet section;
t	is the present temperature;
t_{in}	is the temperature at the boundary between the mixing layer and the vapor cone;
$t_{s \text{ in}}$	is the saturation temperature corresponding to the minimum pressure in the jet, used as the inside boundary isotherm of the mixing layer;
t_∞	is the temperature of the ambient water;
$t_{\text{ou}1}$ and $t_{s \text{ ou}1}$	are the temperatures at the outside boundary of the mixing layer exceeding t_∞ by 0.01 times the total temperature drop in the mixing layer: $t_{\text{ou}1} = t_\infty + 0.01 (t_{\text{in}} - t_\infty)$, and $t_{s \text{ ou}1} = t_\infty + 0.01 (t_{s \text{ in}} - t_\infty)$;
Θ_{to} and Θ_c	are the dimensionless temperatures in the thermal mixing layer: $\Theta_{\text{to}} = (t - t_\infty) / (t_{\text{in}} - t_\infty)$ and $\Theta_c = (t - t_\infty) / (t_{s \text{ in}} - t_\infty)$, respectively;

b_{to} and b_c are the thicknesses of the thermal mixing layer, equal to the distance along the y axis from t_{in} to t_{ou1} and from t_{sin} to t_{sou1} , respectively;
 P_0 is the steam pressure in the nozzle forechamber;
 ΔP is the pressure drop between the water ambient and points in the mixing layer.

LITERATURE CITED

1. J. Böhm, *Gesund. Ing.*, No. 28 (1939).
2. P. A. Vecherskii, "Investigation of the thermal and hydrodynamic phenomena accompanying the outflow of steam into a liquid," in: *Transactions of the Kiev Technological Institute of the Food Industry [in Russian]*, Vol. 3 (1940).
3. F. T. Binford, L. E. Stanford, and C. C. Webster, Oak Ridge National Laboratory, ORNL-4374, UC-80-Reactor Technol. (1968).
4. P. J. Kerney, G. M. Faeth, and D. R. Olson, "Penetration characteristics of a submerged steam jet," *AIChE J.*, 18, No. 3 (1972).
5. B. F. Glikman, "Experimental investigation of the condensation of a steam jet in liquid-filled space," *Izv. Akad. Nauk SSSR, Otd. Tekh. Nauk, Energ. Avtom.*, No. 1 (1959).
6. B. F. Glikman, "Condensation of a steam jet in liquid-filled space," *Izv. Akad. Nauk SSSR, Otd. Tekh. Nauk*, No. 2 (1957).
7. Akio Kudo, Tatsuo Egusa, and Saburo Toda, "Basic study on vapor suppression. Heat transfer," in: *Proceedings of the Fifth International Heat Transfer Conference, Tokyo, 1974*, Vol. 3 (1974).
8. V. E. Nakoryakov and N. S. Safarova, "Simple equation for determining the position of the interface of phases in condensation of a submerged steam jet," *Izv. Sib. Otd. Akad. Nauk SSSR, Ser. Tekh. Nauk*, 8, No. 2 (1975).

INVESTIGATION OF SUBMERGED TURBULENT GAS JETS WITH DIFFERENT DENSITIES

V. A. Golubev and V. F. Klimkin

UDC 532.525.2

The results obtained in measuring the parameters in transverse sections and along the axis of submerged helium, air, and Freon jets are given along with the trends in the variation of the apparent additional mass of these jets.

Although the investigation of turbulent submerged jets has been treated in many papers [1-4], some problems concerning the trends of their propagation have not yet been resolved. We provide here the results of investigations of helium, air, and Freon jets and the generalization of certain characteristics of jets with different densities. Figure 1 shows the distribution of fields of the velocity head $q = \rho U^2/2$, the enthalpy i (or the temperature T), the concentration C (%), and the velocity U in transverse sections of helium, air, and Freon jets, measured in the main part of the jet at distances of 50, 70, 95, 120, and 145 mm from the nozzle cutoff. The jets of the above gases flow into an air atmosphere vertically upward from a profiled nozzle with the diameter $d_j = 5$ mm with fourfold contraction. The parameters of the operating conditions for the investigated jets are given in Table 1.

The velocity head in the jet is measured by means of a total-pressure tube, while the temperature is measured by means of a thermocouple. The concentration of admixtures in the helium jet is measured by means of a receiver with a tungsten filament, which is connected to a resistance bridge circuit.

The velocity U , the density ρ , and the enthalpy i in the jet are determined by measuring the velocity head $\rho U^2/2 = q$, the temperature T , and the concentration C . The Freon concentration by weight is calculated on the basis of measurements of the mixture temperature T_{mi} by means of the relationship [6]

Sergo Ordzhonikidze Moscow Aviation Institute. Translated from *Inzhenerno-Fizicheskii Zhurnal*, Vol. 34, No. 3, pp. 493-499, March, 1978. Original article submitted March 17, 1977.